

Effect of the Passivation Layer on the Noise Characteristics of Mid-Wave-Infrared InAs/GaSb Superlattice Photodiodes

Tunay Tansel, Kutlu Kutluer, Ömer Salihoglu, Atilla Aydinli, Bulent Aslan, Bulent Arikan, Murat Celal Kilinc, Yuksel Ergun, Ugur Serincan, and Rasit Turan

Abstract—The authors describe the noise characterization of a mid-wavelength-infrared (MWIR) photodiode based on indium arsenide and gallium antimonide (InAs/GaSb) superlattice (SL), addressing the influence of different passivation layers applied to the surface of the device. The MWIR InAs/GaSb SL design structure is based on p-i-n configuration grown by the molecular beam epitaxy on a (001) n-GaSb substrate. The SiO₂-passivated SL photodiodes demonstrated a Schottky-limited noise up to a bias voltage of -0.1 V where the measured peak responsivity is 1.37 A/W with a cut-off wavelength of 4.9 μm and the specific detectivity as high as 1.23×10^{12} cm. Hz^{1/2}/W, demonstrating the high quality of the fabricated MWIR SL photodiodes. The noise measurements exhibited a frequency-dependent plateau (i.e., $1/f$ noise) for unpassivated and Si₃N₄-passivated samples, whereas $1/f$ -type noise suppression (i.e., frequency-independent plateau) with a noise current reduction at about 30 Hz of more than one order of magnitude was observed for the SiO₂-passivated ones.

Index Terms—InAs/GaSb, mid-wave-infrared photodiode, noise characterization, passivation.

I. INTRODUCTION

THE Mid-Wavelength-Infrared (MWIR) spectral range from 3 to 5 μm has been playing an important role in different technology fields such as astronomy, medicine, industrial processes and law enforcement. The most used detector material for these applications has been the bulk mercury cadmium telluride (MCT). Infrared detectors based on indium arsenide and gallium antimonide (InAs/GaSb) superlattices (SL) have also been shown to be promising for MWIR applications [1]. The advantage of InAs/GaSb SLs relative to bulk MCT is their strongly suppressed Auger recombination

Manuscript received November 21, 2011; revised January 9, 2012; accepted February 11, 2012. Date of publication February 20, 2012; date of current version April 11, 2012.

T. Tansel, K. Kutluer, and R. Turan are with the Department of Physics, Middle East Technical University, Ankara 06531, Turkey (e-mail: tutansel@metu.edu.tr; kutluer@metu.edu.tr; turanr@metu.edu.tr).

Ö. Salihoglu and A. Aydinli are with the Department of Physics, Bilkent University, Ankara 06800, Turkey (e-mail: omersalihoglu@yahoo.com; aydinli@fen.bilkent.edu.tr).

B. Aslan, B. Arikan, Y. Ergun, and U. Serincan are with the Department of Physics, Anadolu University, Eskişehir 26470, Turkey (e-mail: yergun@anadolu.edu.tr).

M. C. Kilinc is with the Department of Electrical and Electronics Engineering, Middle East Technical University, Ankara 06531, Turkey (e-mail: muratcelalkilinc@gmail.com).

Color versions of one or more of the figures in this letter are available online at <http://ieeexplore.ieee.org>.

Digital Object Identifier 10.1109/LPT.2012.2188504

rates which reduces noise current significantly [2]. However, to enhance the performance of the InAs/GaSb SL photodiodes further, it is essential to have a better understanding of the electrical properties including gain, carrier lifetime, and more significantly, the noise characteristics that should lead one to estimate the *true* specific detectivity (D^*) of the device.

Surface passivation is crucially important for detector operation to suppress the leakage current [3], [4]. This is a performance-limiting factor in the operation of SL infrared detectors. Therefore, we performed direct measurements of the noise spectra for SL diodes based on a p-i-n InAs/GaSb SL design as a function of passivation material to understand the effect of the dark current and noise and their contribution to the detector performance.

II. EXPERIMENT

The MWIR InAs/GaSb SL detector structure is based on 60-periods n-type/60-periods a non-intentionally doped (n. i. d.) active region/90-periods p-type InAs/GaSb SL. Each period in the entire structure consists of 2.85 nm InAs and 3.3 nm GaSb layers with InSb-like interfaces. GaSb layers in the p-type superlattice period were doped with Be to a level of 1.5×10^{17} cm⁻³ while the InAs layers were doped with Te to a level of 5×10^{17} cm⁻³. The entire SL structure was enclosed by a 20 nm n-type InAs: Te (5×10^{17} cm⁻³) top and a 1 μm thick p-type GaSb: Be (1×10^{17} cm⁻³) bottom contact layers. The sample was grown by the crystal growth company IQE Inc. on an n-type (001) GaSb substrate by molecular beam epitaxy (MBE). For ohmic contacts a Ti-Au (30 nm / 300 nm) bi-layer was evaporated onto the top and back surfaces where the unwanted metal was then removed by the lift-off technique.

Passivation was carried out directly after the wet etching (by using a phosphoric and citric acid solution) in order to protect the sample surface from ambient atmosphere: 230 nm silicon oxide (SiO₂) or 150 nm silicon nitrite (Si₃Ni₄) was deposited by Plasma Enhanced Chemical Vapor Deposition (PECVD) at sample temperature of 423 K.

For the dark current and dark noise characterizations, the specimen was placed on a sample holder (cold finger) in a cryostat and cooled down to temperature (T_{sample}) of 79 K using liquid nitrogen. During the measurements, the low noise current amplifier which has also internal bias voltage source (Stanford Research Systems, SR570) was placed inside a shielded box. A rechargeable-battery was used to power up

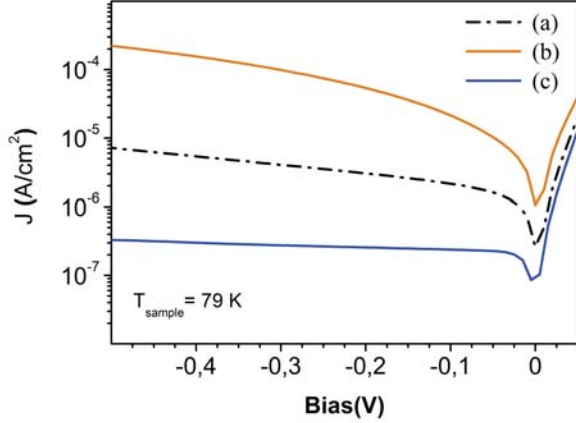


Fig. 1. Dark current density versus applied bias voltage at $T_{\text{sample}} = 79$ K for SL devices (a) with no intentional passivation (unpassivated), (b) passivated by Si_3N_4 , and (c) passivated by SiO_2 .

the voltage source and the amplifier to avoid the effects of the power network. The output signal from the current amplifier was averaged over 500 times by the FFT spectrum analyzer (Stanford Research system, SR760).

For the dark current measurements Keithley (Keithley 2440) source meter was used to apply the DC bias voltage (V_{bias}) to the detector and also to read the output current. In dark current and noise dark current measurements, the complete unit has been controlled via a GPIB (General Purpose Interface Bus) interface.

In order to obtain the intrinsic detector noise, the system noise (i_{sys}) was subtracted from the measured total noise i_{total} (in $\text{A}/\text{Hz}^{1/2}$). The total noise contributions in the measured i_{total} noise can be summarized as follows by assuming that the noise sources are statistically independent [5]

$$i_{\text{total}}^2 = i_{\text{sn}}^2 + i_{\text{jn}}^2 + i_{1/f}^2 + i_{\text{sys}}^2 \quad (1)$$

where $(i_{\text{sn}}^2 + i_{\text{jn}}^2)$ is Schottky-noise $i_{\text{sn}}^2 = 2qI$ and Johnson-noise with $i_{\text{jn}}^2 = 4k_{\text{B}}T/R_{\text{d}}$. Here, k_{B} is the Boltzmann constant, T is the temperature, R_{d} is dark differential resistance, q is the electronic charge constant, and I is the dark current. The current spectral densities of Johnson-noise and Schottky-noise are frequency independent and so are called white noise. The low frequency noise ($i_{1/f}$) is the $1/f$ noise above the white noise level at low frequency, which is inversely dependent on frequency [6]. The $1/f$ noise can be used as an indicator of the device quality [7], [8].

The peak responsivity (as well as the cut-off wavelength) of SLs was calculated from the measured spectral photoresponse by using a calibrated blackbody (Newport, Oriel 67000), [9].

III. RESULTS AND DISCUSSION

Fig. 1 shows the dark current-voltage (I-V) curves at $T_{\text{sample}} = 79$ K for $400\mu\text{m} \times 400\mu\text{m}$ SL diodes with different passivation layers and an unpassivated surface. At reverse bias voltage $V_{\text{bias}} = -0.5$ V, unpassivated and

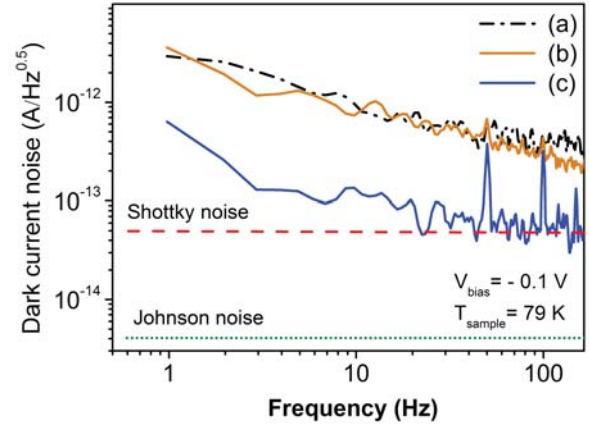


Fig. 2. Noise spectra as function of frequency for (a) unpassivated, (b) passivated by Si_3N_4 , and (c) passivated by SiO_2 samples at $V_{\text{bias}} = -0.1$ V and $T_{\text{sample}} = 79$ K. The peaks in the range of 50–100 Hz are due to electronic noise and their harmonics, respectively.

Si_3N_4 passivated devices exhibit a maximum dark current density of $\sim 10^{-6}$ A/cm² and $\sim 10^{-4}$ A/cm², respectively, while the SiO_2 passivated device shows a clear rectifying characteristic with a dark current density of $\sim 10^{-7}$ A/cm².

For both unpassivated and Si_3N_4 passivated samples, it was found that the dark current density increases with increasing DC bias. The best performance, however, was obtained from the SiO_2 passivated sample where the dark current is one and two orders of magnitude (at the reverse bias of $V_{\text{bias}} = -0.1$ V) smaller compared to unpassivated and Si_3N_4 passivated devices, respectively. The reduction in the dark current indicates that silicon dioxide based passivation layers are likely to be more useful to improve the sample performance, in contrast with Si_3N_4 passivation layers which yields in a relatively higher dark current density, which is in agreement for similar passivant, passivation technique and mesa area to those reported by E. Plis *et al* [3].

In order to understand the above differences in the dark current, the noise performance of the devices are investigated over the frequency range of 1 to 200 Hz at $V_{\text{bias}} = -0.1$ V and $T_{\text{sample}} = 79$ K with the amplifier gain set to 20 nA/V (this leads to the cut off frequency of ~ 200 Hz).

The noise spectra in Fig. 2 shows, for the SiO_2 passivated SL, a frequency independent plateau in the range from 20 to 200 Hz is white noise. This matches with the theoretical calculated Schottky-noise ($i_{\text{sn}} = 5 \times 10^{-14}$ A/Hz^{1/2}) well, thus indicative of a good passivation with the suppression of the $1/f$ noise and a reduction of the dark noise current with one orders of magnitude (at the reverse bias of $V_{\text{bias}} = -0.1$ V) compared to unpassivated and Si_3N_4 passivated devices, respectively. In other words, the influence of dangling bonds and impurities are minimized along the exposed mesa side-walls by the SiO_2 passivation. The presence of the $1/f$ noise contribution confirms that the Si_3N_4 passivated material did not lead to an improvement but rather degradation of the device quality.

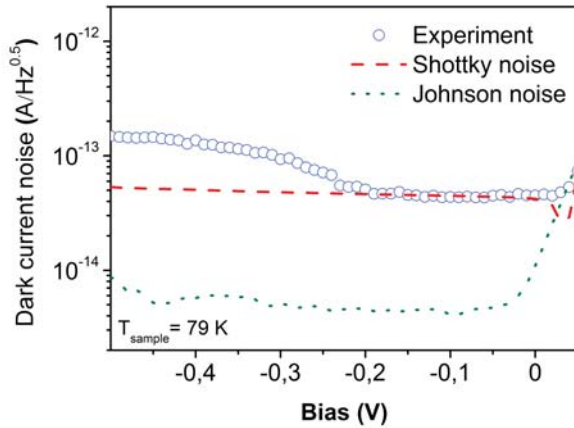


Fig. 3. Total dark noise current as function of the bias at ~ 30 Hz for the SL device passivated with SiO_2 . The dashed line shows the calculated Schottky-noise; the dotted line represents the Johnson-noise.

To extract the intrinsic noise, noise measurements were performed inside the white noise region, namely at 30 Hz, on the same mesa (area of $1.6 \times 10^{-3} \text{ cm}^2$). Fig. 3 shows the measured dark current noise at various bias voltages for the SiO_2 passivated SL diode in comparison to the theoretically calculated curve. Using the measured peak responsivity (R_p) of 1.37 A/W at $4 \mu\text{m}$ ($\lambda_{\text{cut-off}}$ is $4.9 \mu\text{m}$) for $V_{\text{bias}} = -0.1$ V at $T_{\text{sample}} = 79$ K, we calculated the *true* specific $D^* = 1.23 \times 10^{12} \text{ cmHz}^{1/2}/\text{W}$ by using the equation.¹

A further increase of the reverse bias causes a discrepancy between the theoretical calculated Schottky-noise and the experimentally measured noise value at reverse bias voltages below -0.2 V, the experimental value of dark current noise exhibits a sharp contrast with theoretical -Schottky-noise with dark current noise curve becoming higher than the calculated Schottky noise contribution. A discrepancy factor around 3 is observed at $V_{\text{bias}} = -0.5$ V which is in agreement by that reported in Ref. 7. This is due to the fact that, for bias voltage higher than -0.2 V, the $1/f$ noise becomes dominant at 30 Hz. Hence, “*true*” D^* will be significantly different from the theoretical D^* values especially at higher reverse voltages than -0.2 V.

In order to understand its physical reason, we consider the dependence of additional noise upon the bias voltage. It appears that the additional noise depends on the bias voltage. Such voltage dependent additional noise can probably be attributed to very low residual surface leakage currents, which can be related to $1/f$ noise [10]. Conductive oxides of In or Ga cations that may also form at the interface on the mesa side-wall, during the deposition process of SiO_2 passivation layer on the etched SL surface would also decrease the path resistance for surface leakage [7], [11]. Thus, the dominant source of the dark current noise appears to be the additional noise $1/f$ noise encountered at biases smaller (more

¹ $D^* = R_p \cdot \sqrt{A \cdot \Delta f} / i_n$, where, i_n is the dark noise current, Δf is the bandwidth over which the noise is measured, and A is the optical area of device.

negative) than $V_{\text{bias}} = -0.2$ V which degrades the detector performance [11].

IV. CONCLUSION

We studied the dark current and noise in MWIR InAs/GaSb SL devices with and without intentional surface passivation. It was shown that SiO_2 passivation reduces the dark current by up to two orders of magnitude, which is attributed to the effective suppression of surface leakage currents. The noise measurements revealed the absence of intrinsic $1/f$ noise (as well as a noise reduction with one order of magnitude) above 30 Hz and Schottky-limited behavior up to $V_{\text{bias}} = -0.2$ V. Below $V_{\text{bias}} = -0.2$ V a discrepancy was observed between the experimental data and the theoretically expected Schottky-noise, with a factor of ~ 3 . It also introduces additional frequency dependent noise potentially $1/f$ noise probably due to the surface leakage current, resulting in much higher noise in the detector. A further investigation will be done to determine the cause of leakage current by dark current measurement of different mesa size. Furthermore, for the SiO_2 passivated SLs the peak responsivity was found to be 1.37 A/W while the cut-off wavelength was $4.9 \mu\text{m}$ and D^* amounted to $1.23 \times 10^{12} \text{ cmHz}^{1/2}/\text{W}$ at $V_{\text{bias}} = -0.1$ V.

REFERENCES

- [1] S. Mallick, K. Banerjee, S. Ghosh, J. B. Rodriguez, and S. Krishna, “Midwavelength infrared avalanche photodiode using InAs–GaSb strain layer superlattice,” *IEEE Photon. Technol. Lett.*, vol. 19, no. 22, pp. 1843–1845, Nov. 15, 2007.
- [2] E. R. Youngdale, *et al.*, “Auger lifetime enhancement in InAs–Ga_{1-x}In_xSb superlattices,” *Appl. Phys. Lett.*, vol. 64, no. 23, pp. 3160–3162, Jun. 1994.
- [3] E. Pils, *et al.*, “Passivation of long-wave infrared InAs/GaSb strained layer superlattice detectors,” *Infr. Phys. Technol.*, vol. 54, no. 3, pp. 252–257, 2011.
- [4] P.-Y. Delaunay, A. Hood, B. M. Nguyen, D. Hoffman, Y. Wei, and M. Razeghi, “Passivation of type-II InAs/GaSb double heterostructure,” *Appl. Phys. Lett.*, vol. 91, no. 9, pp. 091112-1–091112-3, Aug. 2007.
- [5] K. Jaworowicz, I. Ribet-Mohammed, C. Cervera, J. B. Rodriguez, and P. Christol, “Noise characterization of midwave infrared InAs/GaSb superlattice pin photodiode,” *IEEE Photon. Technol. Lett.*, vol. 23, no. 4, pp. 242–244, Feb. 15, 2011.
- [6] L. Bürkle, F. Fuchs, R. Kiefer, W. Pletschen, R. E. Sah, and J. Schmitz, “Electrical Characterization of InAs/(GaIn)Sb infrared superlattice photodiodes for the 8 to 12 μm range,” in *Proc. Mater. Res. Soc. Symp.*, vol. 607, 2000, pp. 77–82.
- [7] A. Soibel, *et al.*, “Gain and noise of high-performance long wavelength superlattice infrared detectors,” *Appl. Phys. Lett.*, vol. 96, no. 11, pp. 111102-1–111102-3, Mar. 2010.
- [8] L. K. J. Vandamme, “Noise as a diagnostic tool for quality and reliability of electronic devices,” *IEEE Trans. Electron Devices*, vol. 41, no. 11, pp. 2176–2187, Nov. 1994.
- [9] H. Mohseni, E. Michel, J. Sandoen, W. Mitchel, G. Brown, and M. Razeghi, “Growth and characterization of InAs/GaSb photoconductors for long wavelength infrared range,” *Appl. Phys. Lett.*, vol. 71, no. 10, pp. 1403–1405, Sep. 1997.
- [10] S. Mou, J. V. Li, and S. L. Chung, “Surface channel current in InAs/GaSb type-II superlattice photodiodes,” *J. Appl. Phys.*, vol. 102, no. 6, pp. 066103-1–066103-3, 2007.
- [11] M. Herrera, *et al.*, “Atomic scale analysis of the effect of the SiO_2 passivation treatment on InAs/GaSb superlattice mesa side-wall,” *Appl. Phys. Lett.*, vol. 93, no. 9, pp. 093106-1–093106-3, 2008.